The Linnean Society of London ZOOLOGICAL Journal of the Linnean Society

Zoological Journal of the Linnean Society, 2011, **163**, 663–678. With 6 figures

Swima (Annelida, Acrocirridae), holopelagic worms from the deep Pacific

KAREN J. OSBORN[1]*, STEVEN H. D. HADDOCK[2] and GREG W. ROUSE[1]

[1]*Scripps Institution of Oceanography, 9500 Gilman Drive, La Jolla, CA 92093-0202, USA*
[2]*Monterey Bay Aquarium Research Institute, 7700 Sandholdt Road, Moss Landing, CA 95039, USA*

Received 16 September 2010; revised 3 December 2010; accepted for publication 16 December 2010

Two new species of *Swima*, a recently established genus of annelid worms, are introduced, one from deep water off the North American West Coast and the other from the Philippines. The acrocirrid genus now contains three named species, *Swima bombiviridis,* ***Swima fulgida*** **sp. nov.**, and ***Swima tawitawiensis*** **sp. nov.** *Swima* are holopelagic, occurring only in the water column, and thus far have only been observed below 2700 m. The worms are relatively large, sometimes reaching over 30 mm in length and 5 mm in width. They have gelatinous bodies and fans of long swimming chaetae, which are flattened into paddles in ***S. tawitawiensis*** **sp. nov.** Members of *Swima* are distinguished from other swimming acrocirrids by their transparent bodies, single medial subulate branchiae, and simple nuchal organs that do not skirt the bases of lateral subulate branchiae. ***Swima fulgida*** **sp. nov.** is distinguished from other members of the genus by its darkly pigmented anterior gut, whereas ***S. tawitawiensis*** **sp. nov.** is distinguished by possessing three subulate head appendages instead of just one and by the shape of its noto- and neurochaetae. *Swima* species possess four pairs of elliptical, transformed segmental branchiae that produce green bioluminescence when autotomized. These 'bombs' were observed in various states of regeneration on a single individual. *Swima* are neutrally buoyant, often observed hanging immobile in the water column, and are active, agile swimmers. Although not previously documented in the literature, these worms are not rare in the deep water column. Since the worms were first noticed in 2001, they have been observed on more than half of the Monterey Bay Aquarium Research Institute's midwater remotely operated vehicle dives that went to sufficient depth. The discovery of *Swima* underscores our lack of knowledge of deep pelagic fauna.

doi: 10.1111/j.1096-3642.2011.00727.x

ADDITIONAL KEYWORDS: Celebes Sea – Cirratuliformia – deep-sea – gelata – midwater – pelagic – *Swima bombiviridis* – ***Swima fulgida*** **sp. nov.** – ***Swima tawitawiensis*** **sp. nov**.

INTRODUCTION

Increased access to deep water with research submersibles has enabled advances in our understanding of deep-sea animal physiology and behaviour, as well as new appreciation for the importance of gelatinous animals in pelagic communities (Robison, Sherlock & Reisenbichler, 2010). Direct observations have led to the discovery of many previously unknown species that were for so long missed because they were too delicate to be successfully collected by nets or because they could actively avoid capture (Haddock, 2004). Use of submersibles allowed the recent discovery of seven spectacular new species of swimming annelids (Osborn *et al*., 2009).

The recently discovered swimming worms shared features with both Flabelligeridae and Acrocirridae, which are sister groups (Rouse & Fauchald, 1997; Rouse & Pleijel, 2003; Osborn & Rouse, 2010). Understanding of the relationships amongst acrocirrids and flabelligerids is still developing, with several efforts to

*Corresponding author. Current address: Department of Invertebrate Zoology, National Museum of Natural History, Smithsonian Institution, Washington D.C. 20052, USA.
E-mail: osbornk@si.edu

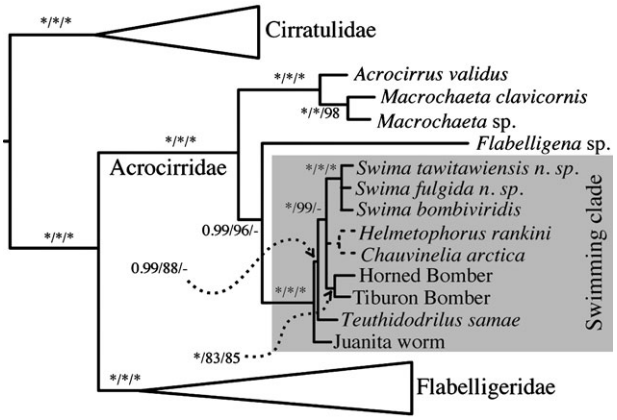

Figure 1. Ninety-five per cent majority rule consensus tree from Bayesian analyses of five concatenated genes [*18S*, *28S*, *16S*, cytochrome oxidase I (*COI*) and cytochrome *b* (cyt*b*)] from cirratuliform annelids, showing *Swima* as part of Acrocirridae (Osborn & Rouse, 2010). Support indicated as posterior probabilities, bootstraps from the maximum likelihood analysis and from the parsimony analysis. Asterisks indicate 1.0 or 100% support.

assess their evolutionary history (Rouse & Pleijel, 2003; Rousset *et al*., 2007; Osborn & Rouse, 2008; Salazar-Vallejo, Carrera-Parra & Fauchald, 2008; Osborn *et al*., 2009). Thus placement of the new species required a phylogenetic study of Cirratuliformia, focused primarily on Flabelligeridae and Acrocirridae (Fig. 1; Osborn & Rouse, 2010). That study found that all seven recently discovered swimming species formed a clade (referred to hereafter as the 'swimming clade') with *Helmetophorus* Hartman, 1978 and *Chauvinelia* Laubier, 1974 and that clade belonged in Acrocirridae. With the addition of *Swima* Osborn *et al*., 2009 and *Teuthidodrilus* Osborn, Madin & Rouse, 2010, Acrocirridae now probably consists of eight genera with just over 40 known species whose members are primarily small, thin benthic worms. The majority of the known acrocirrids were collected from the seafloor, yet even before the discovery of the seven swimming species there was reason to believe certain acrocirrids could swim. *Helmetophorus rankini* Hartman, 1978 and both species of *Chauvinelia* Laubier, 1974, have long chaetae, relatively fragile bodies, and were thought to be demersal (capable of swimming up off the seafloor at times; Hartman, 1978; Averincev, 1980; Kirkegaard, 1982). Additionally, the long capillary chaetae sometimes found in *Acrocirrus* are referred to as 'swimming' chaetae (Banse, 1969), although their ability to swim, like that of *Chauvinelia* and *Helmetophorus*, is unconfirmed. It is possible that some of these records represent epitokous forms that transform for reproductive purposes.

The description of *Swima bombiviridis* Osborn *et al*., 2009 (Fig. 2) and *Teuthidodrilus samae* Osborn *et al*., 2010 confirmed the presence of holopelagic species within Acrocirridae (Fig. 1) and provided the third confirmed evolutionary origin of pelagicism within Cirratuliformia (*Poeobius*, Burnette, Struck & Halanych, 2005; *Flota*/*Buskiella*, Osborn & Rouse, 2008; *Swima*, Osborn *et al*., 2009). Here we describe the two species most closely related to the type species of *Swima, S. bombiviridis*, and restrict the genus to these three species based on morphological and molecular data. We also provide further information on *S. bombiviridis* and notes on behaviour and ecology of *Swima*.

MATERIAL AND METHODS

COLLECTIONS

Three specimens of *Swima fulgida* sp. nov. were collected from deep water off central California over the period 2004 to 2009 (Table 1). All *in situ* observations were made with the Monterey Bay Aquarium Research Institute's (MBARI's) deep-diving remotely operate vehicles (ROVs) *Tiburon* and *Doc Ricketts*, which were equipped with a Panasonic high resolution, three-chip camera or an Ikegami HDL-40 camera attached to a Fujinon BERD HA 10×5.2 lens. Video was recorded on high-quality BetaCam and high definition television tapes for subsequent analysis, and these are housed in the video archive at MBARI. Specimens were captured in 7.5 L detritus samplers or with the high-flow suction sampler (Robison, 1992). Both methods greatly reduce the abrasion and crushing typical of collection in nets, and also provide a way to collect the organism and its surrounding water undisturbed. The relatively large amount of native water collected with each organism additionally serves to insulate the organism against changes in water temperature and chemistry during the trip to the surface. Upon recovery from such great depth, animals were mostly unresponsive unless pinched with forceps or when initially placed in isoosmotic magnesium chloride. Specimens were photographed with a Nikon Coolpix 5000 as macro shots or through a Nikon dissecting scope, prior to fixation.

Specimens were further imaged in the lab using a Canon G9 fitted on a Leica MZ8 stereomicroscope. Some parapodia were removed from specimens and examination via differential interference contrast on a Leica DMR compound microscope with a Nikon Coolpix 4300. Parapodia were then prepared for scanning electron microscope imaging by transfer through buffer and fresh water rinses and an ethanol dehydration series before air drying and mounting. Chaetae were viewed with an FEI Quanta 600 scanning electron microscope.

Table 1. Specimen, collection, and accession numbers. All are hologenophores (Pleijel *et al.*, 2008)

voucher accession and type designation (molecular ID no.)	Collection date	Locality	Collection depth (m)	18S	28S	16S	COI	Cyt*b*	Fixative
Swima bombiviridis									
SIO BIC A1282 holotype (PB51)	7.iv.05	36°19.80′N, 122°53.99′W	3054	GQ422143	GQ422144	FJ944506	FJ944527	FJ944540	Glutaraldehyde
SIO BIC A1281 paratype (PB44)	5.vi.05	36°43.98′N, 123°41.93′W	3744	FJ944493	FJ944516	FJ944505	FJ944526	FJ944539	Glutaraldehyde
n/a (PB39)	22.iii.05	36°19.80′N, 122°53.99′W	3187	FJ944495	–	FJ944508	FJ944529	FJ944542	n/a
SIO BIC A1283 paratype (P9)	28.xi.07	35°50.42′N, 122°40.13′W	3019	FJ944494	FJ944517	FJ944507	FJ944528	FJ944541	Glutaraldehyde
SIO BIC A1284 paratype (PB42)	5.vi.05	36°43.98′N, 123°41.93′W	3744	FJ944496	FJ944518	FJ944509	FJ944530	FJ944543	Glutaraldehyde
SIO BIC A1634 paratype (P31)	21.ix.05	36°19.80′N, 122°53.99′W	3442	–	–	–	**GQ338664**	–	Formalin
SIO BIC A1635 paratype (P26)	20.ix.05	36°19.80′N, 122°53.99′W	3325	–	–	–	**GQ338662**	–	95% ethanol
SIO BIC A1636 paratype (P30)	2.x.06	35°37.99′N, 122°44.00′W	2732	–	–	–	**GQ338666**	–	Glutaraldehyde
SIO BIC A1637 paratype (P25)	2.xi.07	36°19.39′N, 122°54.18′W	3411	–	–	–	**GQ338667**	–	95% ethanol
SIO BIC A1638 paratype (P28)	26.ii.09	35°07.61′N, 122°55.60′W	3600	–	–	–	**GQ338665**	–	95% ethanol
n/a (P23)	22.vi.06	36°20.08′N, 122°55.00′W	3333	–	–	–	**GQ338668**	–	n/a
n/a (P24)	23.vi.06	36°20.08′N, 122°55.00′W	3247	–	–	–	**GQ338663**	–	n/a
SIO BIC A1676 paratype (P27)	26.ii.09	35°07.61′N, 122°55.60′W	3600	–	–	–	**GQ338661**	–	95% ethanol
***Swima fulgida* sp. nov.**									
SIO BIC A1285 holotype (PB32)	7.x.04	35°46.38′N, 122°50.24′W	3267	FJ944497	–	–	FJ944531	FJ944544	Glutaraldehyde
SIO BIC A1286 paratype 1 (P1)	22.vi.06	36°20.08′N, 122°55.00′W	3478	FJ944498	FJ944519	FJ944510	FJ944532	FJ944545	Glutaraldehyde
SIO BIC A1675 paratype 2 (P29)	26.ii.09	35°07.61′N, 122°55.60′W	3625	–	–	–	**GQ338660**	–	95% ethanol
***Swima tawitawiensis* sp. nov.**									
NMA 0437 holotype (P13)	6.x.07	4°58.00′N, 120°14.61′E	2836	FJ944499	FJ944520	FJ944511	FJ944533	FJ944546	Formalin

GenBank numbers in bold indicate previously unpublished sequences.
Fixation methods are indicated for the anterior portion of each type specimen.
Posterior tissue clips were frozen in liquid nitrogen or fixed and preserved in 95% chilled ethanol then used for genomic DNA extraction
COI, cytochrome oxidase I; Cyt*b*, cytochrome *b*; n/a, not applicable.

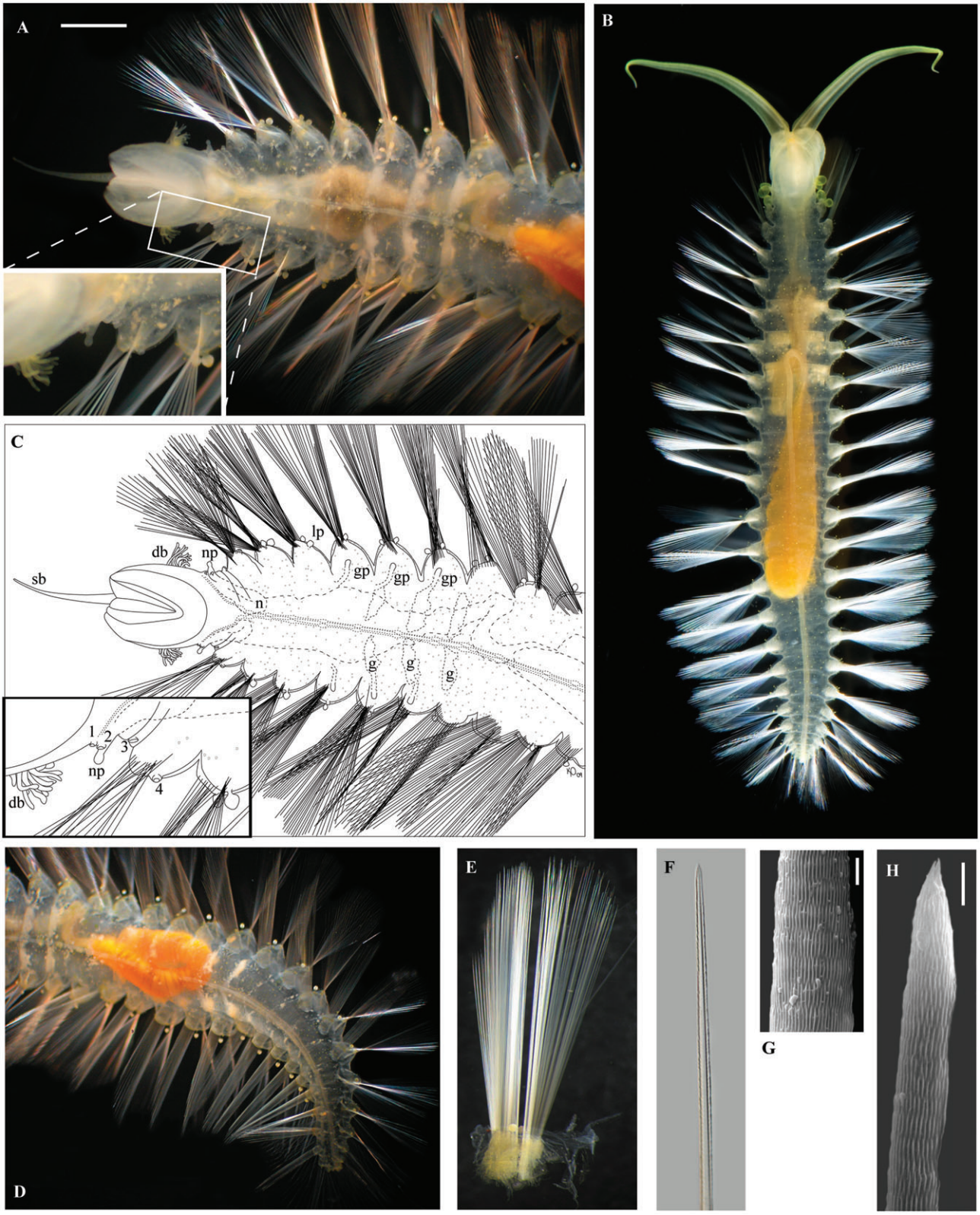
A
B
C
db
np
lp
sb
gp
gp
gp
n
g
g
g
1
2
3
np
4
db
D
E
F
G
H

Figure 2. Compilation of figures reproduced with permission from description of *Swima bombiviridis* (Osborn *et al*., 2009) with the addition of C. Images A, B, and D taken from live animals. A, ventral view of holotype anterior with inset detailing elliptical branchiae scars, digitiform branchiae, and nephridiopore papillus. B, dorsal view of paratype, showing grooved palps, chaetal fans, at least six attached 'bombs', transparent body with gut and gonads visible through body wall, gelatinous sheath, and yellow, clavate papillae projecting through the gelatinous sheath. Photo credit, © Casey Dunn 2007. C, illustration of A showing location of features: lollipop-shaped papillae (lp), gonopores (gp), gonads (g), digitiform branchiae (db), medial subulate branchia (sb), and nephridia (n), nephridiopore papillus (np), and elliptical branchiae scars (1–4 inset). D, ventral view of posterior end showing interramal lollipop-shaped papillae and posterior gut loops. E, parapodium showing notochaetae on right and neurochaetae on left, two interramal lollipop-shaped papillae, and fragments of the gelatinous sheath. F, light micrograph of distal portion of a chaeta. G, scanning electron micrograph of shaft of a chaeta. H, scanning electron micrograph of distal tip of a chaeta. Scale bars: A = 4 mm, G and H = 2 μm.

The only specimen of *Swima tawitawiensis* sp. nov. was observed and collected from the deep water column of the Celebes Sea in October of 2007 by the ROV *Max Rover Global Explorer* operated off the Research Vessel *Hydrographer Presbitero*. The specimen was damaged during collection but retained characters sufficient to distinguish the specimen from its congeners.

Specimens of *Swima* were recovered in varying conditions and preserved using several methods (70 or 95% ethanol, 2% sodium cacodylate buffered glutaraldehyde, 4–20% formalin, or frozen in liquid nitrogen).

DNA sequencing

Specimens of both *S. fulgida* sp. nov. and *S. bombiviridis* have variable morphology with respect to head appendages, presence of gametes and gonopores, visibility of branchial scars, possession of digitiform branchiae, buccal organ morphology, and general body form; thus, as many specimens as possible were sequenced for a fragment of the mitochondrial cytochrome oxidase I (*COI*) gene to determine if there were one or multiple species present. Genomic DNA was extracted from specimens using a Qiagen DNeasy tissue kit (Valencia, CA, USA). Approximately 650 base pairs of the mitochondrial *COI* gene were amplified using universal primers HCO2198 and LCO1490 (Folmer *et al*., 1994). Twenty-five-microlitre reactions were carried out using either Illustra PuReTaq Ready-To-Go PCR beads (GE Healthcare, Uppsala, Sweden) or Promega GoTaq Green (Madison, WI, USA). Amplification profile: five cycles of 94 °C for 30 s, 45 °C for 90 s, 72 °C for 60 s, 30 cycles of 94 °C for 30 s, 51 °C for 90 s, 72 °C for 60 s, initial denaturation at 94 °C for 60 s and final extension at 72 °C for 5 min.

PCR products were sequenced directly after spin column purification (Ultrafree-DA columns, Millipore, Billerica, MA, USA) following the manufacturer's protocols. All sequencing was carried out using the same primers that were used in the amplification. Sequencing was carried out by Advanced Studies in Genomics, Proteomics and Bioinformatics at the University of Hawaii at Manoa using Applied Biosystems BigDye terminator chemistry and an ABI 3730XL sequencer. Sequences have been deposited in GenBank (Table 1).

Phylogenetic analyses

Sequences were aligned with MUSCLE 3.6 (Edgar, 2004) using default settings and proof-read by eye in MacClade v.4.04 OS X (Maddison & Maddison, 2000). Third codon positions were not removed from analyses because no evidence of saturation was found with *COI* following the Xia *et al*. (2003) test implemented in DAMBE (Xia and Xie, 2001). Flabelligeridae were used as the outgroup for this analysis examining the relationships within Acrocirridae because they are the sister group of the Acrocirridae (Rouse & Fauchald, 1997; Rouse & Pleijel, 2003; Osborn & Rouse, 2010). The complete alignment is available from K. J. O. or at TreeBase (http://www.treebase.org/treebase-web/home.html).

Bayesian analyses of the data sets were conducted using MrBayes 3.1.2 (Huelsenbeck & Ronquist, 2001). Standard procedures based on MODELTEST 3.5 (Posada & Crandall, 1998) were implemented in PAUP* 4.0b10 to select the most appropriate model. The relative fit of models was assessed by the Akaike information criterion (AIC). Smaller values of AIC are preferred (Akaike, 1974; Posada & Crandall, 2001) and the general time reversible + proportion invariant + gamma (GTR+I + Γ) represented the optimal model. Partitions were unlinked in all analyses. Each Markov chain, three heated and one cold, was started from a random tree and all four chains were run simultaneously for five to 60 million generations, with trees being sampled such that the resulting data set from each run contained at least 10 000 data points after burn-in. AWTY (Wilgenbusch, Warren & Swofford, 2004) was used to determine if a sufficient number of generations had been completed for posterior probabilities to stabilize, as

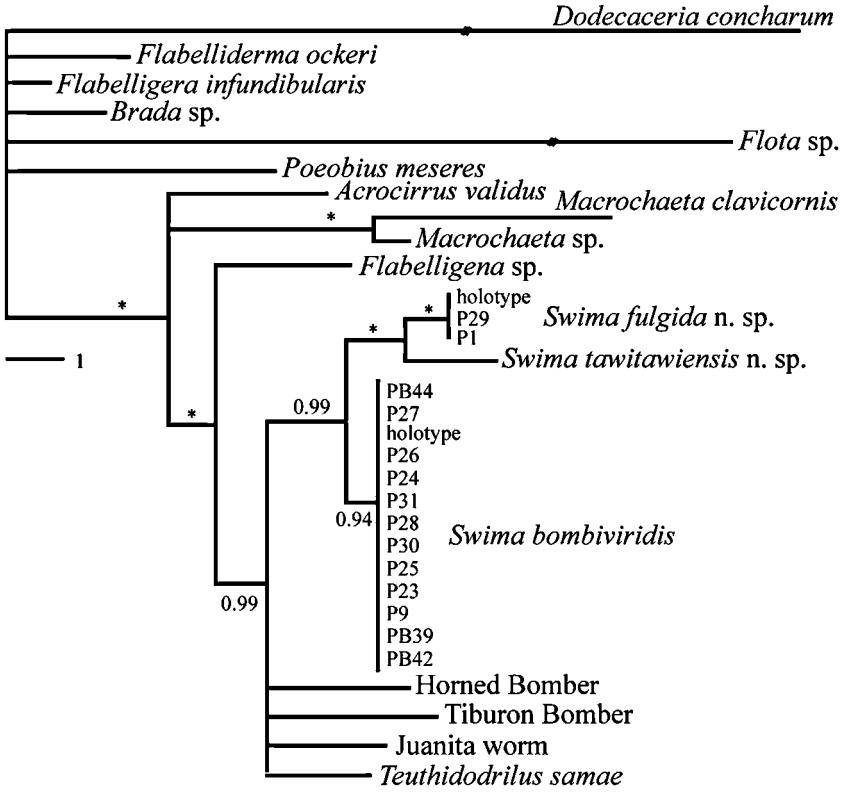

Figure 3. Ninety per cent majority rule consensus cytochrome oxidase I (*COI*) gene tree from Bayesian analyses of cirratuliform annelids, showing *Swima* as part of Acrocirridae and support for *Swima* monophyly. Unsupported branches were collapsed. Support indicated as posterior probabilities. Asterisks indicate 1.0 or 100% support.

well as to determine the amount of required burn-in before inference from the Markov chain Monte Carlo (MCMC) data set was made. Repeated analyses converged on similar parameter estimates.

RESULTS AND DISCUSSION

The swimming clade (Fig. 1) contains acrocirrids with six distinct morphologies (*Swima, Helmetophorus, Chauvinelia*, horned/Tiburon bombers, *Teuthidodrilus*, and Juanita worm). Distinctiveness of each morphology-based group (*Swima*, *Teuthidodrilus*, horned/Tiburon bombers, and Juanita worm were available for molecular analyses) was also observed in sequence data. A well-supported group of three species was recovered within the more inclusive clade originally designated as *Swima* (Osborn *et al*., 2009). This less inclusive clade (*Swima sensu stricto*) contained the type species, *S. bombiviridis*, and two other morphologically similar species, which are described here. *Swima* is here restricted to *S. bombiviridis*, *S. fulgida* sp. nov., and *S. tawitawiensis* sp. nov., which formed a well-supported clade in all molecular analyses (Figs 1, 3). Their transparent body, thick gelatinous sheath, the form of their nuchal organs as a simple ridge with no more than a single 180° bend, small 'bombs' (elliptical branchiae, largest less than half width of body), and possession of a medial subulate branchia distinguish them from all known acrocirrids, including the as-yet-undescribed demersal species (Osborn & Rouse, 2010).

Swima s.s. differed from other sequenced acrocirrids by 16–25% uncorrected pairwise *COI* distance (*18S* 0.7–18%, *28S* 3–13%, *16S* 11–36%, and cytochrome *b* (cyt*b*) 16–30%; see Osborn & Rouse, 2010, for all additional sequencing protocols) and flabelligerids by 18–30% uncorrected pairwise *COI* distance (*18S* 11–20%, *28S* 15–36%, *16S* 23–36%, and cyt*b* 25–33%). *Swima bombiviridis, S. fulgida* sp. nov., and *S. tawitawiensis* sp. nov. differed from each other by 14–16% uncorrected pairwise *COI* distance, from the other members of the swimming clade by 17–22%, and from other acrocirrids by 19–23%. Within-species distances were less than 3% for *COI*. Six unique haplotypes were present amongst the 13 specimens of *S. bombiviridis* sequenced for *COI* with a single haplotype being dominant (7 of 13 specimens). Each of the three specimens of *S. fulgida* sp. nov. had a unique *COI* haplotype.

SYSTEMATICS

SWIMA OSBORN *ET AL.*, 2009

Type species: Swima bombiviridis Osborn *et al*., 2009

Diagnosis (emended): Swimming acrocirrids with thick gelatinous sheath penetrated throughout by long, clavate papillae. Body transparent. One or more lollipop-shaped, inter-ramal papillae projecting well beyond gelatinous sheath. With more than 30 long (more than body width) chaetae per parapodium. Eyes absent. Head not retractable. Nuchal organs just posterior to palps as simple, slightly raised ciliated ridges making no more than single 180° bend, not curving around bases of subulate branchiae. Possessing single, medial subulate branchia either individually or as part of a single row of subulate branchiae immediately posterior to palps and anterior to segmental branchiae, not easily lost. Sometimes with single row of more than 30 digitiform branchiae just posterior to subulate branchiae. Nephridiopores as papillae on second achaetous segment. Four pairs of segmental branchiae modified as ellipsoid, bioluminescent structures, the second of which is attached to basal portion of nephridiopore papillae. Segmental branchiae small (largest less than half width widest body), easily lost, leaving obvious circular scars.

Remarks: Photos for the type species (*S. bombiviridis*, Fig. 2) are reproduced from Osborn *et al*. (2009: supplement), with permission, to represent the characters of the genus and for comparison to the species described here. *Swima* shares the following features with other Acrocirridae: several achaetous anterior segments (Figs 2A, C, 4E, 5B, 6E), shape of prostomium, presence of nephridiopores near second branchiae (Figs 2C, 5B, 6F), gonads in three or fewer anterior segments (Figs 2C, 4E, 5A, 6G), four pairs or fewer of branchiae that are easily lost, and simple, spinous notochaetae (Figs 2E–H, 4G–H, 5F–H, 6B). *Swima* differs from *Macrochaeta* Grube, 1850, *Acrocirrus* Grube, 1873, *Flabelligella* Hartman, 1965, and *Flabelligena* Gillet, 2001 in general body form (Fig. 2A), the absence of eyes, and presence of more than 30 chaetae per parapodium (Figs 2E, 4A, 6C). *Swima* differs from *Flabelliseta incrusta* Hartman, 1978 in the shape of the notopodial papillae, by possessing notochaetae, and by not adhering sediment particles to their gelatinous sheath. *Swima* is similar to *Helmetophorus rankini* Hartman, 1978 and *Chauvinelia* (consisting of *Chauvinelia biscayensis* Laubier, 1974 and *Chauvinelia arctica* Averincev, 1980), sharing with them the nature of their buccal organ and possibly the ability to swim, although the latter is unconfirmed in *Chauvinelia* and *Helmetophorus*. Members of *Swima* differ from members of *Helmetophorus* and *Chauvinelia* by lacking a cephalic hood and elongate achaetous anterior segments, possessing a medial subulate branchia, having simple, not convoluted nuchal organs, and in general body size. *Swima* and *Chauvinelia* further differ from *Helmetophorus* by possessing lollipop-shaped interramal papillae (Figs 2D, 4C) and more than 30 chaetae per parapodium. Although the papillae drawn by Glasby & Fauchald (1991) from the types suggest *Helmetophorus*'s interramal papillae are lollipop-shaped, examination of the type material indicates that they are not because they lack the extremely bulbous, granular appearing, solid distal tips. Instead, *Helmetophorus* has flaccid, nongranular, moderately bulbous distal tips on their clavate interramal papillae.

Analysis of molecular sequences (Figs 1, 3) shows that *Swima* forms a well-supported clade distinct from all previously known acrocirrids and flabelligerids available for these analyses. *Helmetophorus, Chauvinelia*, *Flabelliseta*, and *Flabelligella* were unavailable for genetic analyses, but as detailed above, they are distinguishable from *Swima* based on morphology. *Helmetophorus* and *Chauvinelia* are the most likely of these missing taxa to form a clade with *Swima*, but their morphology clearly distinguishes them from *Swima* as outlined above.

SWIMA FULGIDA SP. NOV.

Green bomber sp. 1 (Osborn *et al*., 2009), shining bomber (Osborn & Rouse, 2010).

Common name: Shining bomber

Type material: Holotype, collected off the central coast of California 7.x.2004 at 3267 m over a bottom depth of 3546 m by K. J. O. and S. H. D. H., deposited at the Benthic Invertebrate Collection of Scripps Institution of Oceanography (SIO BIC A1285; 35°46.38′N, 122°50.24′W). Two female paratypes collected by K. J. O. (SIO BIC A1286, 22.vi.2006, at 3478 m, 36°20.08′N, 122°55.00′W, undetermined live length; A1675, 26.ii.2009, at 3625 m, 35°7.61′N, 122°55.60′W, > 30 mm).

Diagnosis: Member of *Swima* with a darkly pigment anterior gut and buccal organ. Possessing single, subulate, medial branchia, thick, transparent gelatinous sheath penetrated throughout by narrow clavate papillae, simple noto- and neurochaetae, and three achaetous anterior segments supporting ellipsoid, bioluminescence-producing, derived branchiae that are less than 1.2 mm in length.

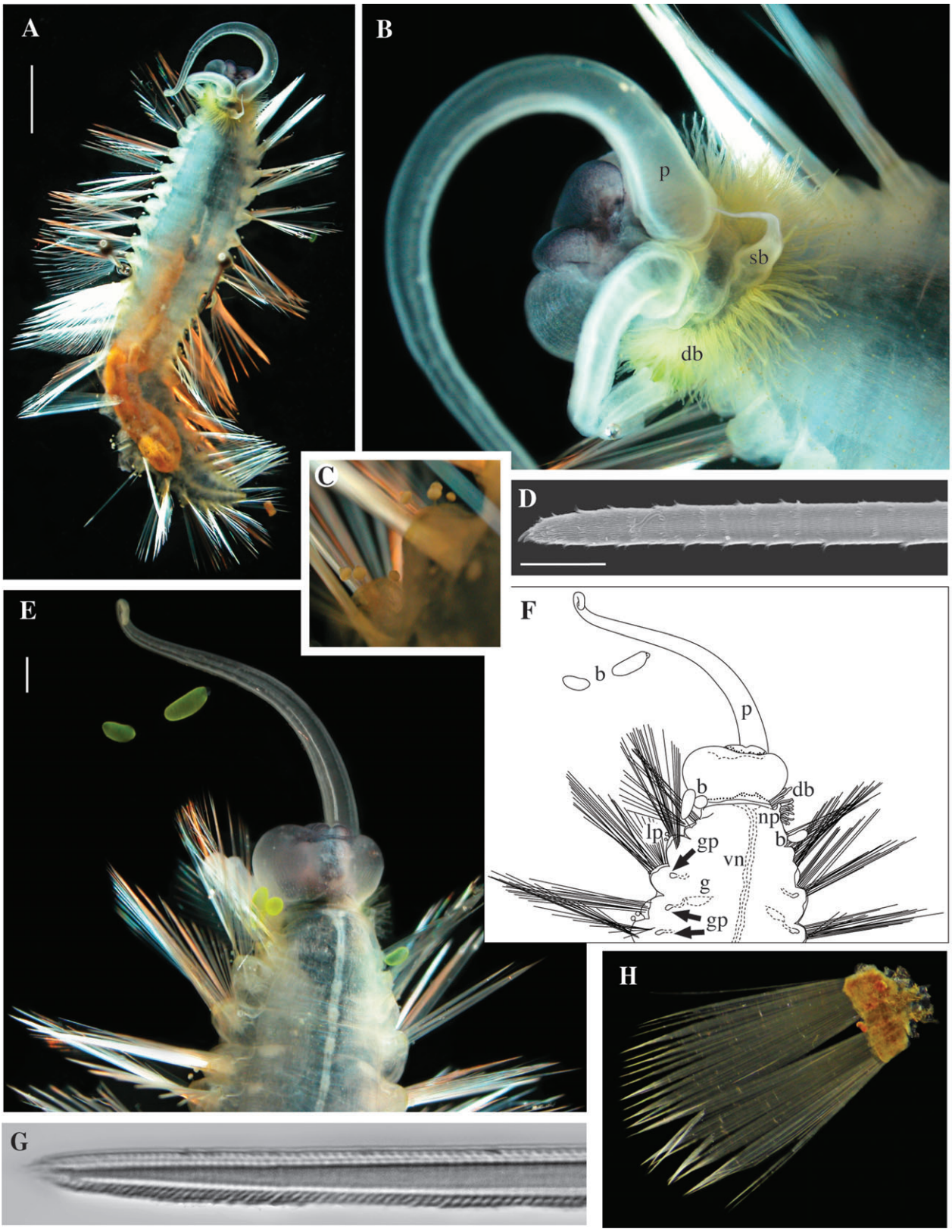
A
B
p
sb
db
C
D
E
F
b
p
b
db
np
lp
gp
vn
b
g
gp
G
H

Figure 4. ***Swima fulgida*** **sp. nov.** holotype. Images A, B and E taken of live animal. A, whole animal dorsal view (pins holding animal down should not be confused with structures on the animal). B, dorsal view of anterior showing yellow digitiform branchiae (db), palps (p), medial subulate branchia (sb), dark pigmented lateral lips of buccal organ, and body papillae as small yellow dots on dorsum. C, ventral view of lollipop-shaped papillae on chaetigers 15 and 16. D, scanning electron micrograph of distal tip of chaeta. E, ventral view of anterior showing the buccal organ, double ventral nerve cord, three autotomized 'bombs' (green) and two attached (right side on first chaetiger, left side on one anterior segments and one recently autotomized) and gonad in early development at the posterior margins of chaetigers 4 and 5. F, illustration of image in E showing location of features. Abbreviations: b, bombs or elliptical branchiae; db, digitiform branchiae; g, gonad; gp, gonopore; lp, lollipop-shaped papillae; np, nephridiopore papilla; p, palp; vn, ventral nerve cord. G, light micrograph of tip of neurochaetae from seventh chaetiger, showing whorls of fine spines. H, seventh chaetiger, notochaetae seen above and neurochaetae below. Scale bars: A = 4 mm, D = 10 μm, E = 1 mm.

Etymology: Named for the shining or gleaming (*fulgidus*) bioluminescence produced by the four pairs of ellipsoid, segmental branchiae. Feminine.

Holotype description: Body transparent, 27 chaetigers, 29 mm live body length, distinct parapodial lobes, numerous long chaetae, posterior half smoothly tapered, broadest segments after chaetiger 3 (Fig. 4A). Thick gelatinous sheath through which narrow, clavate, yellow (in life) papillae, extend (Fig. 4B). Papillae especially numerous on parapodia and dorsum of anterior segments. Pygidium unadorned.

Head consists of prostomium, peristomium, and three achaetous segments possessing what is interpreted here as three forms of branchiae (Fig. 4B, E, but see *Variation*). Prostomium limited to tissue posterior to palps supporting a pair of low, ciliated, oblique ridge-like nuchal organs (shown in paratype 1 Fig. 5C). No eyes. Grooved frontal peristomial palps transparent to yellow in life, tapered, coiling tips, long, reaching at least sixth chaetiger (Fig. 4A). Peristomium surrounds prostomium completely. Buccal organ anteroventrally located, unarmed, bilobed, forming eversible lateral lips. Lateral lips with dark pigment, purple-brown in life, inner lobe transparent to purple-brown in life (Fig. 4B). Slight ridge found posterior to nuchal organs (anterior to digitiform and medial branchiae) possibly indicating a segment margin (Fig. 4B). Three forms branchiae: (1) single, long (reaches to fourth chaetiger), tapered/subulate, medial projection interpreted here as branchia, transparent to white (Fig. 4B) peristomial or on segment 1; (2) more than 40, fine, digitiform respiratory branchiae present across lateral and dorsal surface segment 1 or 2 in tightly packed, single row, yellow in life (Fig. 4B); and (3) three pairs elliptical lobe-like branchiae on achaetous anterior segments (posterior to all other forms branchiae) and one pair on chaetiger 1 (referred to colloquially as 'bombs' because they burst into light when dropped by animal; Fig. 4E, F). Segmentally occurring, elliptical, lobe-like branchiae greenish-yellow in life, autofluorescent, produce green bioluminescence when detached, often autotomized, 0.7 to 1.1 mm in length (Fig. 4E). All elliptical branchiae detached from holotype during collection, examination, and/or storage. Scars from detached elliptical branchiae distinguishable in live and preserved specimen as slightly raised rings thickened tissue, four pairs: one slightly ventral from lateral midline just posterior to digitiform branchiae, one posterior on medial half of nephridiopore papillae, one posterior to nephridiopore papillus at lateral midline, one posterior to chaetae on first notopodium (shown in paratype 1 Fig. 5B).

Chaetigers similar along body. Noto- and neuropodial lobes form continuous, nearly smooth parapodium (Fig. 4H) with more fine papillae relative to rest of body surface. One to four, white to brown, clavate papillae with rounded bulbous tips and narrow bases ('lollipop'-shaped) found between noto- and neuropodial lobes, projecting well beyond gelatinous sheath, tips solid (Fig. 4C). Noto- and neurochaetae indistinguishable except by position, simple, with no articulations (Fig. 4D, G, shown in paratype 1 Fig. 5F). High magnification reveals fine whorls of spines making distal tips appear segmented (Fig. 4D, G, shown in paratype 1 Fig. 5G), bases appear striated. Distal edge of spinous whorls project as frayed edges on worn and longest chaetae (Fig. 4D, shown in paratype 1 Fig. 5H). Chaetigers 4–6 each with a pair of gonopores, low, hollow papillae at ventral base of neuropodia (Fig. 4E, F).

Internal anatomy visible through transparent body wall and gelatinous sheath (Fig. 4A, shown in paratypes Fig. 5A, D). Ventral nerve cord with two paired, fused ganglia in each segment, diverge just posterior to peristomium to surround buccal organ, fused again just posterior to palp attachment points (Fig. 4E, shown in paratypes Fig. 5A, D). Single pair of large, anterior, semitransparent nephridia reaching second chaetiger, largely lying in ventral part of coelum, overlapping each other in ventral portions of first and second chaetigers, folding back anterodorsally, then narrowing, with each nephridium leading to a lateral nephridiopore (shown in paratype 2

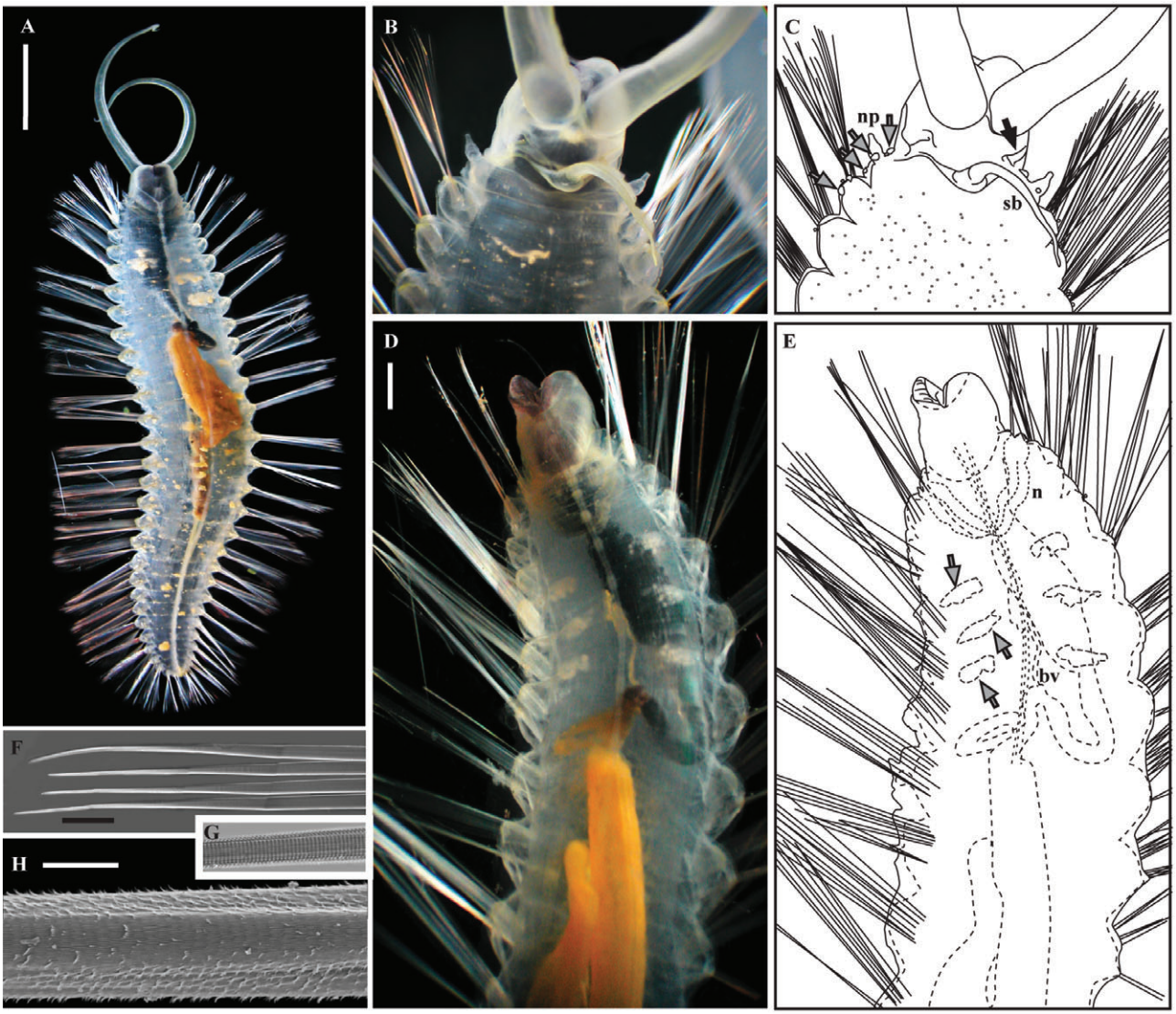

Figure 5. ***Swima fulgida*** **sp. nov.** paratype 1 (A–C, F–H) and paratype 2 (D–E), images A, B, D taken from live animals. A, ventral view, whole animal. Dark pigmented foregut and coils of orange midgut are visible through the transparent body wall. B, dorsal view, anterior. C, illustration showing location of features visible in B. Grey arrows indicate left elliptical branchiae scars; black arrow indicates right nuchal organ. The bases of the palps, the medial subulate branchia (sb), nuchal organs, and nephridiopore papillus (np) are visible. D, ventral view, anterior. E, illustration showing location of features visible in C. Developing gonads indicated by arrows; posterior fold of the left nephridia (n), and dorsal blood vessel (bv) visible. F, light micrograph of notochaetae, stitched compilation of four images. G, light micrograph of shaft of chaeta. H, scanning electron micrograph of shaft of chaeta. Scale bars: A = 5 mm, D = 1 mm, F = 0.4 mm, H = 10 μm.

Fig. 5D–E). Gut running from buccal organ straight for one-third body length (approximately to chaetiger 10) after which a wide, single loop is formed. Gut in this loop portion broadens (to at least one quarter body width) and continues back to approximately chaetiger 20 before narrowing and turning anterior. Gut continues anterior to near first loop then folds rearward and continues directly to pygidium. Foregut (region anterior to the first loop) darkly pigmented, appearing black through body wall, expandable to near body width (Fig. 4A, E, shown in Paratypes Fig. 5A, D, E). Heart body and dorsal blood vessel first distinguishable just posterior to digitiform branchiae, extends through anterior one-third of body until apparently merging with anterior-most dorsum of broadened portion of gut (shown in paratype 2

Fig. 5D, E). Gonads form at posterior margin of chaetigers 4–6 (shown in paratype 2 Fig. 5D, E).

Variation: The two paratypes had 27 and more than 28 chaetigers (specimen incomplete), respectively. Each was more than 30 mm total body length when alive. *Swima* are particularly prone to distortion when injured and to preservation artefacts. If specimens were not completely relaxed prior to fixation, they contracted dramatically during initial fixation. Additionally, when specimens were injured they often contracted around the injury site. The degree of buccal organ lateral lobe eversion varied amongst preserved specimens.

Palps were easily dislodged from specimens during handling leaving obvious scars. Palps varied in length relative to body length. The length of the single, medial branchia also varied in length relative to body length. Digitiform branchiae were not easily lost from the holotype and left obvious scars when they were. Digitiform branchiae were absent from both paratypes genetically confirmed to belong to the species. Elliptical branchiae were easily autotomized, even during the gentlest collection, and were often found on the floor of the sampling device upon recovery of the ROV or were detached during laboratory examination. As no specimens were recovered with all elliptical branchiae attached, it was not possible to determine if more than one pair can be attached to a single segment at one time, but this seems unlikely based on the scars. Various sized elliptical branchiae, ranging from 0.6–1.2 mm in longest dimension, were found on a single individual. Smaller 'bombs' were nearly spherical whereas larger branchiae were ellipsoidal.

Paratype 1 with obvious gonopores only on chaetiger 6 and developing gonads in the right posterior margin of chaetiger 4 and left posterior margin of chaetigers 4–6 (Fig. 5A). Paratype 2 with developing gonads in chaetigers 4–6 (Fig. 5D), obvious gonopores only in chaetiger 5. Oocytes in female up to 0.5 mm in diameter.

Remarks: Swima fulgida sp. nov. is most similar to *S. bombiviridis*. The presence of dark pigment on the foregut and lateral lips of the buccal organ, as well as the differences found in *COI* and cyt*b* sequences clearly separate the two species. Additionally, specimens of *S. fulgida* sp. nov. tend to be larger than those of *S. bombiviridis* and are broadest after the third chaetiger, unlike *S. bombiviridis*, which tapers from the head and first chaetiger. *Swima fulgida* sp. nov. has fewer prominent interramal lollipop-shaped papillae than *S. bombiviridis*. See *Remarks* below for comparison to *S. tawitawiensis* sp. nov.

It cannot be determined at this time if the structures referred to here as subulate and digitiform branchiae are peristomial or segmental. Unlike other branchiae known in acrocirrids and flabelligerids (Spies, 1975), these structures are not easily detached. The digitiform branchiae were not lost from the two paratypes by handling or damage to the specimen; they were absent. Absence of digitiform branchiae was also observed in *S. bombiviridis* where specimens were observed with numerous long, few short, or absent digitiform branchiae. Pulling on both digitiform and subulate branchiae of both live and dead specimens resulted in breakage of the structure at various positions along their lengths and left ragged, torn edges. This contrasts with the removal of palps and elliptical lobe-like branchiae, which always come away from the body at the base and leave a regular, sealed scar.

The spherical tips of the lollipop-shaped papillae found in *S. bombiviridis* and *S. fulgida* sp. nov. should not be confused with the balloon-like tips of the notopodial papillae of *Flabelliseta incrusta*. The tips of the lollipop-shaped papillae are solid, with a granular outer appearance whereas the balloon-shaped papillae are described as hollow with a smooth outer surface.

Ecology: Swima fulgida sp. nov. was found off of the central California coast at 3267–3625 m depth, from 30–340 m above the seafloor. Similar animals were observed via ROV but not collected (identification unconfirmed) off the Oregon coast (45°24.02′N, 126°43.00′W), as well as the Gulf of California (24°18.99′N, 109°11.95′W) by K. J. O. Animals were not observed on the seafloor although they were sometimes observed within sight of it via the ROV. The proximity to the seafloor at great depth, ability to swim, and delicate body are probably the reasons why this species was only recently discovered.

Animals were observed hanging horizontally in the water column with the dorsal surface uppermost and the palps hanging forward and downward over the buccal organ, which typically projects anteroventrally. *Swima fulgida* sp. nov., like others in the clade, swims by lateral undulation of the body coupled with expansion on the power stroke and contraction on the recovery stroke of the chaetal fans. Observations of parapodia removed from the animal suggest that this expansion and contraction of chaetal fans can be attributed to passive mechanical mechanisms, not requiring musculature. Swimming was observed to be both forward and rearward, which was difficult to distinguish unless the ROV was completely still and camera zoomed in enough to identify the anterior end. Animals were seldom observed *in situ* in close enough detail to determine the direction of their initial

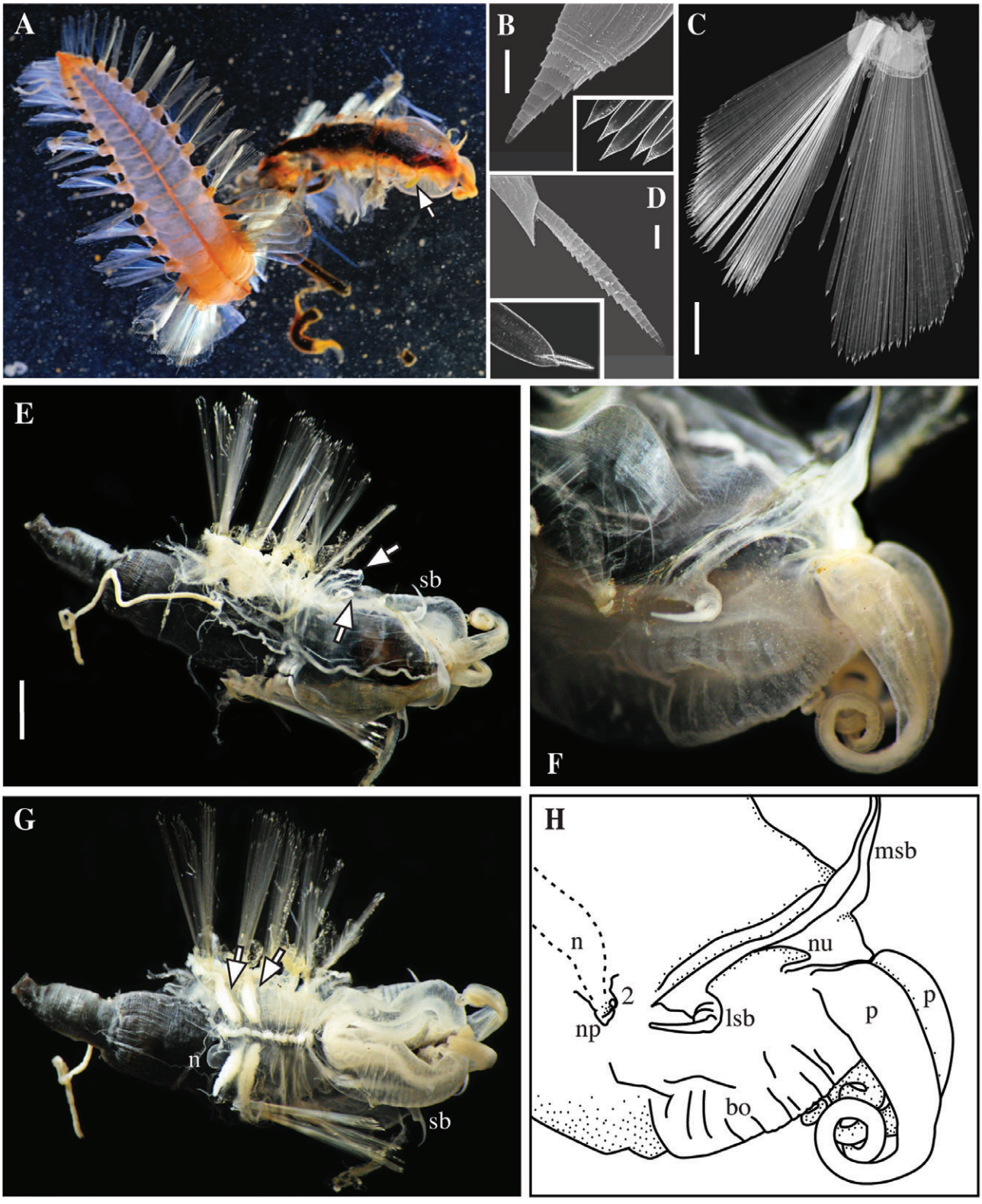
A
B
C
D
E
sb
F
G
n
sb
H
msb
n
nu
2
np
lsb
p
p
bo

Figure 6. ***Swima tawitawiensis*** **sp. nov.** holotype. A, ventral view of posterior portion and twisted laterodorsal view of anterior portion upon recovery from the remotely operated vehicle. Arrow indicates an attached bomb. B, scanning electron micrograph of notochaeta tip; inset, differential interference light micrograph of several notochaetae. C, parapodium with notochaetae on right and neurochaetae on left. D, scanning electron micrograph of neurochaeta tip; inset, differential interference light micrograph of neurochaeta. E, dorsolateral view, anterior fragment of the preserved specimen showing palps, subulate branchiae (sb indicates left lateral branchia), peeled away gelatinous sheath around bases of chaetae, and the outgrowths of body wall supporting the two posterior-most elliptical branchiae scars (arrows). F, right lateral view of head. G, ventral view anterior fragment of preserved specimen showing gonads in chaetigers 4–5 (arrows), posterior fold of left nephridium (n), buccal organ, coiled palps, shape of the left lateral subulate branchia (sb), and the dark gut wall. H, illustration of image in F showing location of features. Abbreviations: 2, second elliptical branchia scar on nephridiopore papillus; bo, buccal organ; lsb, lateral subulate branchia; msb, medial subulate branchia; n, nephridium; np, nephridiopore papillus; nu, nuchal organ; p, palp. Scale bars: B = 50 μm, C = 1 mm, D = 20 μm, and E = 3 mm.

swimming when disturbed, but in the instances where it was possible, it was consistently rearward. This is consistent with the direction of escape swimming observed in other *Swima* species. A rearward escape response is also consistent with use of anteriorly located, autotomizable, bioluminescent decoys by removing the bulk of the body away from the released body part or decoy.

Specimens were recovered in various conditions and possessed from two to eight elliptical branchiae of various sizes. The first pair of elliptical branchiae differed slightly from all other pairs in that the first pair was always smaller than, or the same size as, the smallest bomb found on an individual. The second to fourth bombs varied in size; this was assumed to be because of regeneration of previously autotomized bombs. Manual stimulation of animals at any point along the body or head resulted in release of a bomb or two, which immediately produced green bioluminescence. Further stimulation would result in release of additional bombs if available. Bioluminescence was seen as a steady glow from bombs that had been autotomized. Bombs that were separated from the animal could be triggered to produce light again by gently squeezing them with forceps. The glow of an individual bomb lasted several seconds.

SWIMA TAWITAWIENSIS SP. NOV.

Common name: Orange bomber

Type material: Holotype, and only specimen, collected from the Celebes Sea off Tawi-Tawi, Philippines (4°58.00′N, 120°14.16′E), x.2007 at 2836 m by 'Exploring the Inner Space of the Celebes Sea 2007 Expedition' using ROV *Max Rover Global Explorer* operated from R/V *Hydrographer Presbitero*. Body severed into two pieces when recovered from ROV (anterior fragment, head to chaetiger 5, posterior fragment, 27 chaetigers and pygidium; Fig. 6A). The specimen is deposited at the National Museum of the Philippines (NMA 0437, Table 1).

Diagnosis: Swima with nuchal organs forming oblique lines, each with medial end curved into U-shape. Three equally long, subulate branchiae just posterior to nuchal organs, one medial, with smooth sides, two lateral with 90° projection one-third to one-half distance from base. Notochaetae broad and flattened with a fine, spinous tip. Compound neurochaetae with short (barely as long as the medial element is wide), straight, round in cross section, spinous distal element and broad flattened medial element.

Etymology: Named after the location where it was collected, Tawi-Tawi, Philippines. The locality name is simplified and the adjectival ending *-ensis* is added.

Holotype description: Body transparent (Fig. 6A). Chaetigers with distinct parapodial lobes and numerous long chaetae, posterior body smoothly tapered (Fig. 6A), with gelatinous sheath through which narrow, short, clavate papillae extend. Gelatinous sheath mostly peeled from body, visible as shreds around bases of chaetae. Total preserved body length greater than 45 mm (anterior fragment 15 mm, posterior fragment 30 mm) and 6 mm widest width. Pygidium unadorned.

Head consists of prostomium, peristomium, at least three achaetous segments possessing two forms of branchiae, not retractable (Fig. 6F). Prostomium is tissue posterior to palps supporting nuchal organs. Nuchal organs raised ciliated ridges forming oblique lines with medial ends curved into U-shape (Fig. 6F, H). No eyes. Peristomium surrounds prostomium completely. Grooved frontal palps transparent to orange in life, tapered, coiling at tips, reaching to first chaetiger (Fig. 6E). Buccal organ anteroventrally

located, unarmed, bilobed, forming eversible lateral lips, inner lobe transparent to black (Fig. 6G). Slight ridge found posterior to nuchal organs and anterior to row subulate branchiae, indicating segment margin (Fig. 6F). Two branchial forms: (1) single row of three equally long (to second segment), subulate, transparent to white, single medial with smooth sides, lateral pair with 90° projection one-third to one-half distance from base (Fig. 6E–H), and (2) elliptical branchiae. Photograph taken immediately after collection shows an elliptical branchia attached to the right nephridiopore papillus (Fig. 6A), no elliptical branchiae retained with preserved specimen. Branchial scars lateral, first slightly ventral of lateral midline just posterior to row subulate branchiae, second on medial half of nephridiopore, third and fourth on following achaetous segments on saclike projections of body wall (Fig. 6E). Branchial scars found in the same locations and identical to those in *S. bombiviridis* and *S. fulgida* sp. nov. except the fourth, which is located on an additional achaetous segment instead of on first chaetiger. Elliptical branchiae yellow-green in life. Large projection supporting fourth elliptical branchia scar on left (Fig. 6E top arrow).

Chaetigers undifferentiated into thoracic and abdominal. Noto- and neuropodial lobes form single, nearly smooth projection (Fig. 6C). One to four clavate papillae lollipop-shaped, found between noto- and neuropodial lobes (Fig. 6C). Notochaetae simple with smooth body, no articulations, broad and flat, paddle-like, narrow abruptly to fine point at distal tip (Fig. 6B). Neurochaetae compound, with broad, flat medial element, cylindrical distal element (Fig. 6D). High magnification reveals fine whorls of spines making distal tips noto- and neurochaetae appear segmented (Fig. 6B, D), bases appear striated under high magnification. Chaetigers 4–5 with developing gonads, gonopore low, broad papilla just posterior to right fifth neuropodium.

Internal anatomy visible through transparent body wall and gelatinous sheath. Ventrally located double nerve cord with two pairs fused ganglia per segment, diverge just posterior to peristomium to surround buccal organ, fused again just posterior to palp attachment. Single pair of large anterior, semitransparent nephridia reaching back to fifth chaetiger, ventrally orientated from lateral origin, folding back anteriorly, then narrowing to lead to lateral nephridiopores (Fig. 6F). Gut running from buccal organ straight for one-third body length, coiled in mid-region, straight in posterior region. Anterior gut black, expandable to near body width (Fig. 6E). Heart body and dorsal blood vessel extend through anterior one third of body. Gonads ventral in chaetigers 4–5 (Fig. 6G), chaetiger 6 severely damaged so unknown if contained gonads as well.

Remarks: This species is most similar to *S. fulgida* sp. nov. and *S. bombiviridis* and is sister to the former based on DNA sequence data (Figs 1, 3). *Swima tawitawiensis* sp. nov. possesses a pair of lateral subulate branchiae, which is absent in both other species (Fig. 6F). We suggest that the medial subulate and the lateral projections are branchiae because of the large afferent and efferent blood vessels that run their length and originate from just anterior to the heart body. These structures possess no obvious sensillae. All three projections appear to originate from a single achaetous segment because a slight ridge of tissue connects them (Fig. 6F). Horned and Tiburon bombers, *Chauvinelia* spp. and *Helmetophorus rankini* have similar subulate structures, but possess multiple rows or segments of them, each row possessing various numbers of projections. Each of those species also possesses convoluted nuchal organs that wind along the bases of the subulate branchiae, further distinguishing them from *S. tawitawiensis* sp. nov.

The broad, flattened notochaetae and compound neurochaetae further differentiate *S. tawitawiensis* sp. nov. from *S. fulgida* sp. nov. and *S. bombiviridis* and the other members of the swimming clade, as do the less pronounced interramal lollipop-shaped papillae and U-shaped medial end of the nuchal organs. *Swima tawitawiensis* sp. nov. and *S. fulgida* sp. nov. share a darkly pigmented foregut. The posterior-most pair of elliptical branchiae scars of *S. tawitawiensis* sp. nov. is not on the first chaetiger as found in the other two *Swima* species, but instead they lie on an additional achaetous segment. The body-wall projections supporting the small ring-like scars where the elliptical branchiae were attached also differentiate *S. tawitawiensis* sp. nov. from the other two *Swima* species.

There was variation from one side of the specimen to the other with respect to the form of the posterior-most elliptical branchia scars; this appears to be an abnormal enlargement of the tissue because nothing of the sort was found on the other side of the animal or on any specimens of the closely related species *S. fulgida* sp. nov. and *S. bombiviridis*. No digitiform branchiae were found on the holotype but they might be expected to occur on additional specimens of this species considering the variation found in the other *Swima* species.

In all *Swima* species, the broadened and coiled region of the midgut is always the first portion of the body to deteriorate upon collection (possibly because of release of digestive enzymes when damaged or dying). The gut of *S. tawitawiensis* sp. nov. is presumably coiled similar to that of *S. fulgida* sp. nov. and *S. bombiviridis*, but this could not be determined from the specimen because the body wall was severely damaged, with the gut spilled out.

Ecology: Found in the Celebes Sea at 2836 m depth within 30 m of the seafloor. Animals were not observed on the seafloor. The specimen was dead upon recovery and not checked for bioluminescence.

ACKNOWLEDGEMENTS

We would like to thank Bruce Robison of the Monterey Bay Aquarium Research Institute for ship time made available for observation and collection of several specimens. Thanks go to Larry Madin of Woods Hole Oceanographic Institution, the science party, and crew aboard the R/V *Hydrographer Presbitero* for their work in the Celebes Sea, for the foresight to collect, photograph, and preserve for morphology and molecular work the single specimen of *S. tawitawiensis* considered here. Thanks go to the crew of the R/V *Western Flyer*, the pilots of the ROVs *Tiburon* and *Doc Ricketts*, and the MBARI video lab staff for their dedication to deep-sea exploration. We also thank Cynthia Claxton (UC Irvine) for advice regarding Latin usage and form, although any errors are the sole responsibility of the authors. Evelyn York's expertise on the SEM was much appreciated. Scripps Institution of Oceanography funded K. J. O. and G. W. R. and the University of California President's Postdoctoral Fellowship supported K. J. O. The David and Lucile Packard Foundation provided funding to the Monterey Bay Aquarium Research Institute. The National Geographic Society, National Oceanic and Atmospheric Administration, and Woods Hole Oceanographic Institution provided funding for the Celebes Sea Expedition.

REFERENCES

Akaike H. 1974. New look at statistical model identification. *IEEE Transactions on Automatic Control* **19:** 716–723.

Averincev VG. 1980. *Chauvinelia arctica*, sp. n. (Acrocirridae, Polychaeta) from the Canadian plain. *Issledovaniya fauny morei. Zoologicheskii Institut Akademii Nauk USSR* **25:** 57–62.

Banse K. 1969. Acrocirridae n. fam. (Polychaeta Sedentaria). *Journal of the Fisheries Research Board of Canada* **26:** 2595–2620.

Burnette AB, Struck TH, Halanych KM. 2005. Holopelagic *Poeobius meseres* ('Poeobiidae,' Annelida) is derived from benthic flabelligerid worms. *Biological Bulletin* **208:** 213–220.

Edgar RC. 2004. MUSCLE: multiple sequence alignment with high accuracy and high throughput. *Nucleic Acids Research* **32:** 1792–1797.

Folmer O, Black M, Hoeh R, Lutz R, Vrijenhoek R. 1994. DNA primers for amplification of mitochondrial cytochrome c oxidase subunit I from metazoan invertebrates. *Molecular Marine Biology and Biotechnology* **3:** 294–299.

Gillet P. 2001. *Flabelligena amoureuxi* new genus, new species (Polychaeta, Acrocirridae) from Crozet Islands (Indian Ocean). *Bulletin of Marine Science* **68:** 125–131.

Glasby CJ, Fauchald K. 1991. Redescription of Helmetophorus rankini Hartman, 1978 (Polychaeta: Helmetophoridae) and its transfer to the Flabelligeridae. *Proceedings of the Biological Society of Washington* **104:** 684–687.

Grube AE. 1850. Die Familien der Anneliden. *Archiv für Naturgeschichte, Berlin* **16:** 249–364.

Grube AE. 1873. Die Familie der Cirratuliden. *Jahres-Bericht der Schlesiche Gesellschaft fuer vaterlandische Cultur, Breslau* **50:** 59–66.

Haddock SHD. 2004. A golden age of gelata: past and future research on planktonic ctenophores and cnidarians. *Hydrobiologia* **530/531:** 549–556.

Hartman O. 1965. Deep-water benthic polychaetous annelids off New England to Bermuda and other North Atlantic areas. *Occasional Papers of the Allan Hancock Foundation* **28:** 1–378.

Hartman O. 1978. Polychaeta from the Weddell Sea quadrant, Antarctica. *Antarctic Research* **26:** 124–223.

Huelsenbeck JP, Ronquist F. 2001. MRBAYES: Bayesian inference of phylogenetic trees. *Bioinformatics* **17:** 754–755.

Kirkegaard JB. 1982. The Polychaeta of West Africa Part I. Sedentary species. *Atlantide Report* **5:** 7–117.

Laubier L. 1974. *Chauvinelia biscayensis* gen. sp. nov., un Flabelligeridae (Annélide Polychète Sédentaire) aberrant de l'étage abyssal du Golfe de Gascogne. *Bulletin de la Société Zoologique de France, Paris* **99:** 391–399.

Maddison DR, Maddison WP. 2000. *Macclade*. Sunderland, MA: Sinauer Associates.

Osborn KJ, Haddock SHD, Pleijel F, Madin LP, Rouse GW. 2009. Deep-sea, swimming worms with luminescent 'bombs'. *Science* **325:** 964.

Osborn KJ, Madin LP, Rouse GW. 2010. The remarkable Squidworm is an example of discoveries that await in deep, pelagic habitats. *Biology Letters* **7:** 449–453.

Osborn KJ, Rouse GW. 2008. Multiple origins of pelagicism within Flabelligeridae (Annelida). *Molecular Phylogenetics and Evolution* **49:** 386–392.

Osborn KJ, Rouse GW. 2010. Phylogenetics of Acrocirridae and Flabelligeridae (Cirratuliformia, Annelida). *Zoologica Scripta* **40:** 204–219.

Pleijel F, Jondelius U, Norlinder E, Nygren A, Oxelman B, Schander C, Sundberg P, Thollesson M. 2008. Phylogenies without roots? A plea for the use of vouchers in molecular phylogenetic studies. *Molecular Phylogenetics and Evolution* **48:** 369–371.

Posada D, Crandall KA. 1998. Modeltest: testing the model of DNA substitution. *Bioinformatics* **14:** 917–918.

Posada D, Crandall KA. 2001. Selecting the best-fit model of nucleotide substitution. *Systematic Biology* **50:** 580–601.

Robison BH. 1992. Midwater research methods with MBARI's ROV. *Marine Technology Society Journal* **28:** 32–39.

Robison BH, Sherlock RE, Reisenbichler KR. 2010. The bathypelagic community of Monterey Canyon. *Deep-Sea Research II* **57:** 1551–1556.

Rouse GW, Fauchald K. 1997. Cladistics and polychaetes. *Zoologica Scripta* **26:** 139–204.

Rouse GW, Pleijel F. 2003. Problems in polychaete systematics. *Hydrobiologia* **496:** 175–189.

Rousset V, Pleijel F, Rouse GW, Erséus C, Siddall ME. 2007. A molecular phylogeny of annelids. *Cladistics* **23:** 41–63.

Salazar-Vallejo SI, Carrera-Parra LF, Fauchald K. 2008. Phylogenetic affinities of the Flabelligeridae (Annelida, Polychaeta). *Journal of Zoological Systematics and Evolutionary Research* **46:** 203–215.

Spies RB. 1975. Structure and function of the head in flabelligerid polychaetes. *Journal of Morphology* **147:** 187–207.

Wilgenbusch JC, Warren DL, Swofford DL. 2004. AWTY: a system for graphical exploration of MCMC convergence in Bayesian phylogenetic inference. Available at http://ceb.csit.fsu.edu/awty

Xia X, Xie Z. 2001. DAMBE: Data analysis in molecular biology and evolution. *Journal of Heredity* **92:** 371–373.

Xia XH, Xia Z, Salemi M, Chen L, Wang Y. 2003. An index of substitution saturation and its application. *Molecular Phylogenetics and Evolution* **26:** 1–7.